

Long Range Bond-Bond Correlations in Dense Polymer Solutions

J.P.Wittmer¹, H.Meyer¹, J.Baschnagel¹, A.Johner¹, S.Obukhov^{1,2}, L.Mattioni³, M.Muller⁴ and A.N.Semenov¹

¹Institut Charles Sadron, 6 Rue Boussingault, 67083 Strasbourg, France

²Department of Physics, University of Florida, Gainesville FL 32611, USA

³LPM CN, Université Claude Bernard & CNRS, Lyon, France

⁴Institut für Physik, Johannes Gutenberg-Universität, Staudinger Weg 7, D-55099 Mainz, Germany
(Dated: May 23, 2019)

The scaling of the bond-bond correlation function $C(s)$ along linear polymer chains is investigated with respect to the curvilinear distance, s , along the flexible chain and the monomer density, ρ , via Monte Carlo and molecular dynamics simulations. Surprisingly, the correlations in dense three dimensional solutions are found to decay with a power law $C(s) \sim s^{1-\beta}$ with $\beta = 3/2$ and the exponential behavior commonly assumed is clearly ruled out for long chains. In semidilute solutions, the density dependent scaling of $C(s) \sim g^{1-\beta}$ with $\beta_0 = 2 - 2\alpha = 0.824$ ($\alpha = 0.588$ being Flory's exponent) is set by the number of monomers $g(\rho)$ contained in an excluded volume blob of size ρ . Our computational findings compare well with simple scaling arguments and perturbation calculation. The power-law behavior is due to self-interactions of chains on distances $s \gg g$ caused by the connectivity of chains and the incompressibility of the melt.

PACS numbers: 05.40.Fb, 05.10.Ln, 61.25.Hq

In this Letter we study the correlations of the directions of bonds along polymer chains in semidilute solutions and melts [1, 2, 3, 4]. The problem and some useful notations are sketched in Fig. 1. We focus on flexible monodisperse chains of N monomers under good solvent conditions in three dimensions ($d = 3$) where both the bond length l and the excluded volume screening length R_e are always much smaller than the chain end-to-end distance R_e . In principle, once the bond-bond correlations are computed all other conformational single chain properties can be derived. Importantly, being the (second) derivative of the spatial distances along the chains, they allow us to probe directly | without trivial ideal contributions | the non-gaussian corrections proposed recently [5]. As we shall see, these corrections are crucial to make the description of dense polymer systems, first proposed by Flory [3] and later corroborated by Edwards [2], fully self-consistent.

The bond-bond correlation function $C(s)$ is generally believed to decrease exponentially [3]. This belief is based on the few simple single chain models which have been solved rigorously [3, 4, 6] and on the assumption that all long range interactions are negligible on distances larger than R_e due to the screening mechanism described by Edwards [2]. Hence, only correlations along the backbones of the chains are expected to matter and it is then straightforward to work out that an exponential cut-off is inevitable due to the multiplicative loss of any information transferred recursively along the chain [4].

We demonstrate here that this assumption is in fact incorrect and that unexpected long range correlations remain. They are responsible for a scale free power law regime with $C(s) = c_a(s) s^{-1-\beta}$ for $g(\rho) \ll s \ll N$ ($g(\rho)$ being the number of monomers per blob at monomer density ρ) characterized by an exponent $\beta > 1$ and a density

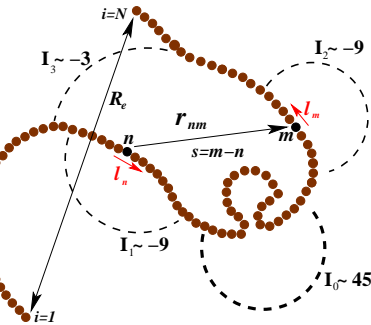


FIG. 1: Sketch of the bond-bond correlation $h_{n \rightarrow m \rightarrow n+1}$ of the bond vectors $l_k = r_{k+1} - r_k$, r_i being the position vector of monomer i . (The two bond vectors are not drawn to scale.) The bond-bond correlation function is defined as the average $C(s) = h_{n \rightarrow n+1} s^{-1-\beta}$ over all possible bond pairs with curvilinear distance $s = m - n \geq 0$ normalized by the mean squared bond length $\langle l^2 \rangle = \langle r_{n+1}^2 \rangle - \langle r_n^2 \rangle$ [7]. The typical size of the corresponding chain segments is $R(s) = \langle r_{nm}^2 \rangle^{1/2}$ with $r_{nm} = r_m - r_n + s$. Note that the end-to-end distance is $R_e = R(s = N - 1)$. The dashed lines show the four relevant graphs of the analytical perturbation calculation. The numerical factors indicate the relative weights of the leading $1/s^{3-\beta}$ contributions to $C(s)$.

dependent amplitude. Our simulation results are presented first and discussed together with simple scaling arguments. We focus on the scale free limit and finite chain size effects ($s \ll N$) are considered more briefly. The analytical calculation (summarized graphically in Fig. 1) is outlined at the end of paper.

Two standard simulation methods for coarse-grained polymer chains [8] have been used to equilibrate long flexible polymer chains for which the bond-bond correlation functions presented in Figs. 2, 3 and 4 below have been computed. The body of our data comes from the "bond fluctuation model" (BFM) {a lattice Monte Carlo

scheme where a monomer occupies 8 lattice sites (i.e., the volume fraction is 8%) and the bonds between adjacent monomers can vary in length and direction, subject only to excluded volume constraints and entanglement restrictions [8, 9]. Using a mixture of local, slithering snake and double-bridging moves [8, 10] we have created ensembles with chain lengths ranging up to $N = 2048$ for densities between $\rho = 0.00195/8$ to $\rho = 0.5/8$ contained in large periodic boxes of linear size $L = 512$ Å which allows us to eliminate finite-size effects. As can be seen in Fig. 2 we have also studied single chains up to $N = 32768$ in an infinite non-periodic box ($\rho = 0$) to characterize properly the dilute reference. Additional molecular dynamics simulations of the bead-spring model discussed in [8] have been performed to check explicitly that our results are not caused by lattice artifacts. As shown in Fig. 4 for one example with $N = 256$ and $\rho = 0.83$, identical behavior (although with reduced statistics) has been found.

Bond-bond correlation functions for different densities are presented in Fig. 2 where we focus first on the behavior of long chains ($s \ll N$). In the dilute limit ($\rho = 0$) the athermal BFM chains are well fitted by $R(s) = b_0 s$, $\beta = 0.588$ being Flory's good solvent exponent and $b_0 = 3.0$. The power law slope with $\beta = \beta_0 = 2/2 = 0.824$ and $\alpha = (2 - 1)/2 = 1/2$ observed in this limit (dashed line) is in fact expected [11] from the formula

$$h_{n,m} = h_{0,n} r_n h_{0,m} r_m \propto \frac{1}{2} \theta_n \theta_m r_{nm}^2 \quad (1)$$

expressing $C(s)$ as the second derivative of $R(s)$. It is crucial that $\beta > 1$ and, hence, $\beta_0 < 1$, i.e. the integral over the correlation function is dominated by its upper bound. Otherwise, β could not be governed by the exponent describing the asymptotic chain size. Interestingly, it follows also directly from Eq. (1) for ideal gaussian chains ($\beta = 1 : c_a = 0$) without additive power law corrections that $C(s)$ must decrease stronger than any power law, i.e. exponentially.

Coming back to Fig. 2, we note that also for finite densities $C(s)$ coincides with the dilute power law for small curvilinear distances s where each chain segment interacts primarily with itself. At larger $s = g()$ where the chains overlap and form a "blob of blobs" the correlation function decreases much faster, however not exponentially as one might expect, but with a second power law regime with $\beta = 3/2$ (bold lines). For the BFM the density $\rho = 0.5/8$ corresponds to a polymer melt since the excluded volume size becomes of order of the average bond size [8]. We observe indeed that the dilute slope disappears in the melt limit and the correlation function can be fitted (bottom bold line) over nearly two orders of magnitude by

$$C(s) = c_a s^{\beta} \quad \text{with } \beta = 3/2; c_a = \frac{P}{4} \frac{6}{\beta^3} \quad (2)$$

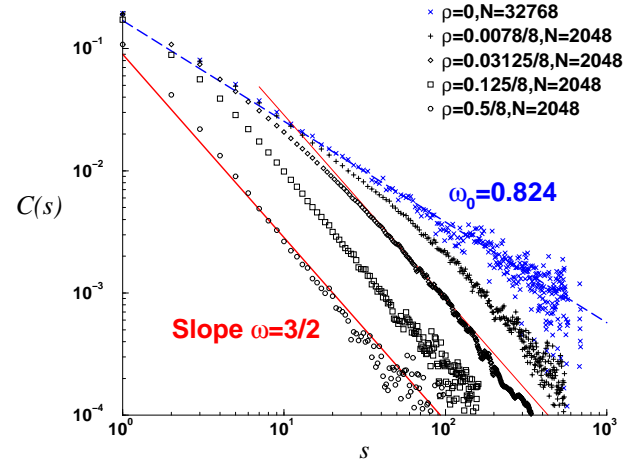


FIG. 2: The bond-bond correlation function $C(s)$ for BFM systems of different densities as indicated in the key. The two lines indicate power laws corresponding to the asymptotic regime for dilute ($\beta_0 = 0.824$, dashed line) and dense ($\beta = 3/2$, bold lines) solutions, respectively. The observation of the second power law regime is the central result of this work. For systems in the so-called semi-dilute regime where the excluded volume is sufficiently large both exponents can be seen. The curvilinear distance at the crossover corresponds to the number of monomers per blob $g()$.

where we anticipate the analytical prediction for the asymptotic scale free limit. Considering that all parameters are known the agreement is excellent although a slightly better fit could be obtained by accepting a larger exponent. Obviously, the chain statistics in the semi-dilute and melt regime must become in leading order gaussian, i.e. the integral over Eq. (1) must be dominated by the lower bound in agreement with the finding $\beta > 1$. In fact, Eq. (2) is consistent with

$$R(s)^2 = b_e^2 s \frac{2c_a l^2}{(\beta - 1)(2 - \beta)} s^{\beta - 1} \quad (3)$$

with $b_e^2 = l^2 \int_{s=0}^{P/2} C(s) ds$ being the statistical segment length of an asymptotically long chain [2]. As long as $\beta < 2$, the correction term (being due to an upper integration bound) contributes a negative, but ever decreasing contribution to the chain distance, i.e., $R_s^2 = s$ approaches b_e^2 from below. Interestingly, Eq. (3) shows that the computation of $C(s)$ allows to highlight directly corrections to gaussian behavior which can be blurred by the large ideal term if moments of spatial distances are considered.

The scaling of the bond-bond correlation function with density and the density dependence of the prefactor c_a are analyzed in Fig. 3. Following the classical density crossover scaling [1] the natural scaling variable is $x = s/g()$ and the figure checks, hence, the scaling

$$C(s)g()^{\beta_0} = f(x) \quad x^{\beta_0}, x^{\beta_0 - 1} : \quad (4)$$

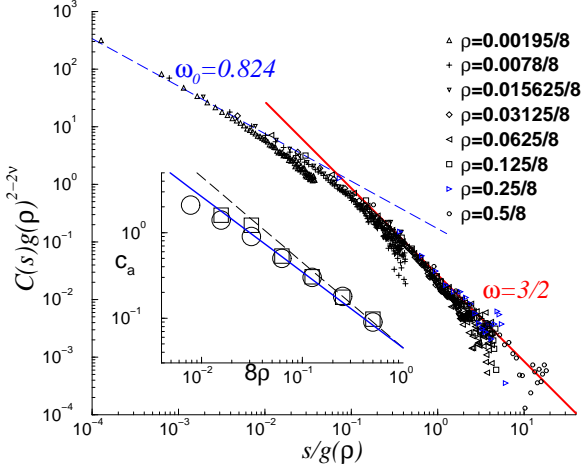


FIG. 3: Crossover scaling for $C(s)$ for BFM model ($N = 2048$) for different densities. In the main panel, the rescaled bond-bond correlation function $f(x) = C(s)g(p)^{1/(1-3/(N-1))}$ is plotted versus the natural scaling variable $x = s/g(p)$ assuming $g(p) \sim p^{1/(1-3/(N-1))}$. Note that for large $s=N$ the natural cut-off (see Eq. (5)) becomes visible. In the inset we explicitly verify the density dependence of the amplitude $C_a(p)$ obtained from $C(s)$ (spheres) and $R(s)$ (squares) using Eq. (2) and Eq. (3) respectively. The prediction for the melt regime, Eq. (2), is indicated by the dashed line, the scaling $C_a(p) \sim p^{1/(1-3/(N-1))} \sim p^{0.885}$ for the semidilute regime by the bold line.

This is well borne out by the data. To be specific, we have used $g(p) \sim p^{1/(1-3/(N-1))}$ [13] although the power law form cannot hold strictly for large densities where the semidilute blobs become too small and the assumed density dependence must be a crude estimate. Considering this, the scaling collapse for all densities (obtained without any arbitrary shift parameter) is far from obvious and quite satisfactory. The amplitude $C_a(p)$ of the non-gaussian corrections has been fitted directly from $C(s)$ and $R(s)$ assuming $1 = 3/2$. As can be seen in the inset, the data compares rather well with the semidilute regime prediction $C_a(p) \sim p^{1/(1-3/(N-1))} \sim p^{0.885}$.

In the following we concentrate on dense melts. In Fig. 4 chain length effects are discussed at constant density. Data from the bead-spring model has also been included to demonstrate the universality of the result. To collapse this correlation function on the BFM data it has been vertically shifted by the ratio of the amplitudes C_a calculated from Eq. (2) for BFM and bead-spring model. As can be seen for $N = 16$, exponentials are compatible with the data of short chains. (This might explain how the power law scaling has been overlooked in previous numerical studies since good statistics for large chains ($N > 1000$) has only become available recently.) However, it is clearly shown that $C(s)$ approaches systematically the scale free asymptote with increasing N . The departure from this limit is fully accounted for by the theory if chain end effects are carefully considered (dashed

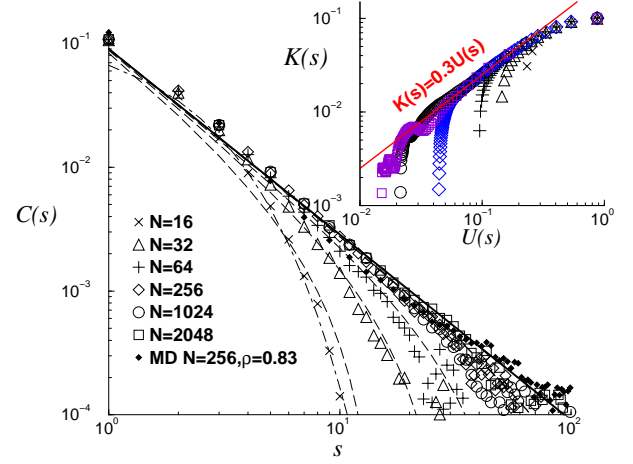


FIG. 4: Bond-bond correlation function versus s at melt densities for different chain length N for the BFM ($p = 0.5/8$) and the bead-spring model ($p = 0.83$) for $N = 256$. The bold line indicates Eq. (2) with $C_a = 0.09$ for long BFM chains. The dashed-dotted curve $C(s) \sim \exp(-s/1.5)$ shows that exponential behavior is compatible with the small N data. The dashed lines correspond to the complete theoretical prediction Eq. (5) for finite chain lengths $N = 16, 32, 64$ and 256 (from left to right). Considering that the theory does not allow for any free fitting parameter the agreement is good. In the inset we check directly the recursion relation Eq. (6) by plotting $K(s)$ versus $U(s) = s = R(s)^3$ (same symbols as in main figure). The proportionality of $K(s)$ and $U(s)$ is well confirmed (bold line) by our data for $1 \leq s \leq N$.

lines). Generalizing Eq. (2), perturbation theory yields

$$C(s) = C_a s^{3/2} a(x) + C_b s^{1/2} b(x) \quad (5)$$

where we have set $x = \frac{s}{N}$ and $C_b = 4C_a/N$ and defined the functions $a(x) = b(x)(1 + 3x + x^2)$ and $b(x) = (1 - x)^2/(1 + x)$. For $x \ll 1$ only the first term contributes, however, as $x \gg 1$ both terms become of similar magnitude. Both contributions to the correlation function vanish rigorously in this limit, and $C(s) \sim (1 - x)^2$.

We outline now very briefly how Eqs. (2) and (5) have been obtained using perturbation calculation [14]. Closely following Edwards [2] we first determine r_{nm}^2

$r_{nm}^2 = \langle 1 + h \cdot i_0 \rangle = r_{nm}^2 U_0$ and then using Eq. (1) the bond-bond correlations. Here, $h \cdot i_0$ denotes the average for the distribution function R_N^k $\int_{R_N^k} dk \int_0^R dk_1 v_1(r_{k1})$ the perturbation potential. The simplest approximation [2] for the effective pair interaction potential is $v_1(r) = v(r) \exp(-r/l) = (4\pi r^2)^{1/2}$ with v being the bare excluded volume and $l = (l^2 = 12\pi v)^{1/2}$ the screening length. This is sufficient for the calculation of the scale free regime (Eq. (2)) and the calculation is straightforward. The graphs which contribute to $h \cdot i_0$ and their relative weights are indicated in Fig. 1. Note that the interactions described by the strongest graph I_0 align the bonds l_1 and l_m while the others tend to reduce the effect.

More care is needed to describe properly the finite chain size corrections (Eq.5). The Padé approximation for the static structure factor must be used here for the interaction potential to obtain a sufficient description for small wave length.

Since these calculations are lengthy we present a simple scaling argument for the β exponent which captures the central physical idea [5]. As suggested by Eq. (3) a direct measure for the non-gaussian corrections can be defined by $K = \frac{R^2(2s)}{2R^2(s)} = \frac{2R^2(s)}{(2R^2(s))} \propto s^{1-d}$ where we compare the size of a segment of length $2s$ with the size of two segments of length s joined together. Equivalently, this can be read as a measure for the swelling of a chain where initially the interaction energy U between the two halves has been switched on. Obviously, K must be a functional of U and $K(U=0) = 0$. Perturbation theory tells us that the lowest order of the expansion of K in U must be linear. What is still missing is an estimate for the scaling of the interaction energy between the segments. For incompressible melts it is well known [1] that the energy penalty for joining two chains of length N is set by the depth of the correlation hole, $U(N) \propto N^{-d}$ [5, 12]. This generalizes to arbitrary s . Hence, in $d=3$ the interaction energy is small ($U(s) \propto s^{-2}$) which finally justifies the perturbation calculation. Taking everything together we obtain $\beta = d = 3=2$ and the important recursion relation

$$K(s) = \frac{R^2(2s)}{2R^2(s)} \quad U(s) \propto s^{-2} \quad (6)$$

The recursion relation provides a very compact and entirely self-consistent description of dense polymer melts ($d > 2$). To lowest order it leads to Eqs. (2) and (3). This shows that while the chain configurations must be gaussian to leading order, corrections do necessarily occur even for very long chains. Eq. (6) has been directly validated in the inset of Fig. 4 where we have plotted $K(s)$ versus $U(s)$. The predicted linearity is well confirmed for large segments ($s \gg 1$). Obviously, the recursion relation being independent of the total chain length N does not capture the scaling for very large segments. The breakdown of the scale free behavior for $K(U)$ (inset) and $C(s)$ (main figure) are both due to the same finite chain size effect.

In summary, we have shown that long range correlations exist in polymer melts and semidilute solutions due to both chain connectivity and incompressibility. Their most striking effect is the power law asymptote for the bond-bond correlation function allowing a direct numerical test [15] of the non-gaussian corrections suggested by the self-consistent recursion relation Eq. (6). Finally, we point out that the physical mechanism which has been sketched above is rather general and should not be altered by details such as a finite persistence length | at

least not as long as nematic ordering remains negligible. This is in fact confirmed by preliminary and on-going simulations.

We thank J.-L. Barrat and K. Binder for useful discussions and acknowledge financial support from LEA and ESF SUPERNET as well as computational resources by IDRIS, Orsay.

Electronic address: jwittmer@ic.ac.uk

- [1] P.-G. de Gennes, *Scaling Concepts in Polymer Physics*, (Cornell University, Ithaca, N.Y., 1979).
- [2] M. Doi and S.F. Edwards, *The Theory of Polymer Dynamics* (Clarendon Press, Oxford, 1986).
- [3] P. J. Flory, *Statistical Mechanics of Chain Molecules*, (Oxford University Press, New York, 1988).
- [4] M. Rubinstein, R.H. Colby, *Polymer Physics*, (Oxford University Press, Oxford, 2003).
- [5] A.N. Semenov, A. Johner, *Eur. Phys. J. E.* 12, 469 (2003).
- [6] O. Kratky, *Rec. Trav. Chim.* 68, 1106 (1949).
- [7] It is also common to use the correlation function of the normalized bond vectors $\mathbf{l} = \mathbf{j}_2 - \mathbf{j}_1$.
- [8] J. Baschnagel, J.P. Wittmer, H. Meyer, Monte Carlo Simulation of Polymers: Coarse-Grained Models, in *Computational Soft Matter: From Synthetic Polymers to Proteins* edited by N. Attig et al. (NIC Series, Volume 23, Julich, 2004), pp. 83-140.
- [9] I. Carmesin and K. Kremer, *Macromolecules*, 21, 2819 (1988); H.P. Dutsch and K. Binder, *J. Chem. Phys.*, 94, 2294 (1991); W. Paul, K. Binder, D. Heermann and K. Kremer, *J. Phys. II*, 1, 37 (1991).
- [10] R. Auhl, R. Everaers, G.S. Grest, K. Kremer and S.J. Plimpton, *J. Chem. Phys.* 119, 12718 (2003).
- [11] E. Eisenberg, A. Baram, *J. Phys. A: Math. Gen.* 36 (2003) L121-124.
- [12] Interestingly, U does not depend explicitly on the excluded volume parameter v . The scaling of $U(r;N)$ has been verified directly by measuring the pair correlation function $g_{cm}(r)$ of the chain center of masses and using $\exp(-U(r;N)) \propto g_{cm}(r) = g_{cm}(1)$.
- [13] The prefactor has been obtained from the scaling of $R(s)$ for densities $\rho < 0.125 = 8$. The crossover from dilute to dense behavior occurs at the surprisingly low value $s = g(1) = 0.06$. Apparently, the mutual chain interactions do not only show up much stronger in $C(s)$ ($\beta = 0.824 \neq 3=2$) compared to $R(s)$ ($\beta = 0.588 \neq 1=2$), but also much earlier. The prefactor difference is explained by the fact that $R(s) = \sum_{k=0}^{\infty} (s-k)C(k)dk$ is an integral strongly dominated by short distances where $C(s)$ decays like in dilute solutions.
- [14] A similar description has been also obtained for polydisperse living polymers using the polymer magnetic analogon. This will be presented elsewhere.
- [15] The same behavior is also found for the second Legendre polynomial. This is important since this quantity may allow to probe experimentally the non-gaussian corrections.